

Article

# The Moisture Diffusion Equation for Moisture Absorption of Multiphase Symmetrical Sandwich Structures

Hang Yu <sup>1</sup> , Lu Yao <sup>1,\*</sup>, Yan Ma <sup>2</sup>, Zhaoyuan Hou <sup>1</sup>, Jiahui Tang <sup>1</sup>, Yuming Wang <sup>1</sup> and Yang Ni <sup>3</sup>

<sup>1</sup> School of Transportation and Civil Engineering, Nantong University, Nantong 226019, China; yuhang@ntu.edu.cn (H.Y.); 2033110073@stmail.ntu.edu.cn (Z.H.); 18020322606@163.com (J.T.); wangyuming@ntu.edu.cn (Y.W.)

<sup>2</sup> School of Textile and Clothing, Nantong University, Nantong 226019, China; mayan0416@ntu.edu.cn

<sup>3</sup> Shanghai Electro-Mechanical Engineering Institute, Shanghai 201109, China; bruceinyang@163.com

\* Correspondence: yaolu@ntu.edu.cn; Tel.: +86-18862898166

**Abstract:** When hydrophilic materials (such as natural fiber, epoxy resin or concrete) compose sandwich structures, the moisture absorption from hydrothermal environments may significantly affect their mechanical properties. Although some experimental works were carried out, few mathematical efforts have been made to describe the moisture diffusion of multiphase symmetrical sandwich structures thus far. In this paper, the moisture diffusion equation was developed to effectively predict the moisture diffusion behavior of multiphase symmetrical sandwich structures as the function of aging time. Both finite element analysis (FEA) and experimental works were carried out to validate the accuracy of the analytical method, and the analytical results show a good agreement with FEA and experimental data. The effect of the interface condition on the concentration at the interfaces was discussed; the difference between concentration and normalized concentration was illustrated; the correct interface condition, which is a continuous normalized concentration condition, was explained for the moisture diffusion behavior of sandwich structures.



**Citation:** Yu, H.; Yao, L.; Ma, Y.; Hou, Z.; Tang, J.; Wang, Y.; Ni, Y. The Moisture Diffusion Equation for Moisture Absorption of Multiphase Symmetrical Sandwich Structures. *Mathematics* **2022**, *10*, 2669. <https://doi.org/10.3390/math10152669>

Academic Editor: Giancarlo Consolo

Received: 30 June 2022

Accepted: 25 July 2022

Published: 28 July 2022

**Publisher's Note:** MDPI stays neutral with regard to jurisdictional claims in published maps and institutional affiliations.



**Copyright:** © 2022 by the authors. Licensee MDPI, Basel, Switzerland. This article is an open access article distributed under the terms and conditions of the Creative Commons Attribution (CC BY) license (<https://creativecommons.org/licenses/by/4.0/>).

**Keywords:** sandwich structures; moisture diffusion equation; normalized concentration; multiphase

**MSC:** 35Q74

## 1. Introduction

Sandwich structures have been widely used in daily life and engineering, such as automotive, sport equipment, building and aerospace, since they present good energy absorption properties, lightweight characteristics, and good designability [1–4]. Despite these advantages, if the materials used in the sandwich structures are hydrophilic materials, they have the drawback of high hydrophilicity when they are exposed to hydrothermal environments [5–7]. The moisture in the environment will diffuse into the sandwich structures and then affect the mechanical property of the materials until the failure of the structures [8–11]. The analysis of the moisture diffusion behavior of sandwich structures is important for their long-term performances and future applications [12–14]. Thus, an effective method should be developed to predict their moisture diffusion behavior.

Some experimental and numerical works have been carried out to study the moisture diffusion behavior of sandwich structures. For example, Saidane et al. [15] investigated the moisture absorption of flax/glass composite sandwich structures. It is found that if glass fiber layers increase, the water uptake and speed of diffusion will obviously reduce. Nurge et al. [16] investigated the moisture diffusion of a graphite/epoxy composite sandwich coupon with a foam core. They developed a finite-difference method by applying a mass-conserving approach to accurately predict the moisture uptake, and a good agreement was achieved with the experimental results. Katzman et al. [17] studied the moisture diffusion behavior of polymer core materials in sandwich structures. A similar

finite-difference method was developed to predict the moisture uptake as a function of time. It is found that this method agreed well with the experimental results. Jalghaf [18] developed the numerical method to solve similar equations, and a comparative study of explicit and stable time integration schemes was carried out.

Although the experimental works have been done on the moisture diffusion behaviors of sandwich structures [19–22], few analytical works have been done to describe their moisture diffusion behaviors, especially for sandwich structures which have a multiphase structure. Yu and Zhou [23] studied two-phase moisture diffusion equations for the moisture diffusion behaviors of flax/glass fiber reinforced composites. The analytical calculations show a good agreement with FEA and experiment results. Joshi et al. [24] solved the moisture diffusion problem of sandwich structures. They used continuous moisture concentration conditions, which are treated as the simplest interface conditions. The form of interface condition between different phases can significantly affect the final results of the moisture absorption [25,26].

Comparative studies of the heat conduction and moisture diffusion problem were presented in some of the literature [27–30]. It should be noticed that when we solve the heat conduction problem, the temperature at the interface of sandwich structure is continuous, however, the concentration at the interface is discontinuous. This important difference is pointed by some studies [25,31]. According to the correct one, the interface conditions should be modified to continuous normalized concentration conditions, otherwise the analytical solution will be totally different from the real situation. Bao [31] discussed the moisture absorption of composite materials, and the moisture diffusivity models were developed according to continuous normalized concentration condition. They also indicated that the relative moisture concentration should correspond to temperature rather than absolute concentration.

From the literature review, the studies on moisture diffusion in two-phase symmetrical sandwich structure have been developed. However, research on moisture diffusion of multiphase symmetrical sandwich structures, which are important materials in engineering, is seldom found in references. In this paper, the moisture diffusion equation is developed to solve moisture diffusion behaviors of multiphase symmetrical sandwich structures. Firstly, the moisture diffusion problem was solved using continuous normalized concentration interface conditions. Then, both FEA and experimental works were introduced and carried out. Finally, the analytical results were compared with FEA and experiment results to validate the proposed analytical method. Moreover, the effects of different interface conditions on the moisture diffusion behavior of sandwich structures were also discussed.

## 2. Method

The diagram of multiphase symmetrical sandwich structure is shown in Figure 1a, and the moisture is applied at the upper and bottom surfaces of sandwich structure. To investigate moisture diffusion along the thickness direction, this moisture diffusion problem is simplified as shown in Figure 1b, where the white layer, grey layer and blue layer are defined as Phase 1, Phase 2 and Phase 3. The saturated moisture concentration  $C_\infty$  is defined as  $C_\infty = M_\infty/V$ , where  $M_\infty$  is saturated moisture uptake and  $V$  is volume of the sample [32]. The saturated moisture concentrations and diffusivities of phase 1–3 are  $C_{1\infty}$ ,  $D_1$ ,  $C_{2\infty}$ ,  $D_2$ ,  $C_{3\infty}$  and  $D_3$ , respectively. The thicknesses of phases 1–3 are  $a_1-a_2$ ,  $a_2-a_3$  and  $a_3$ , respectively, and  $C_1(x,t)$ ,  $C_2(x,t)$  and  $C_3(x,t)$  represent the moisture concentrations in phases 1–3, where  $t$  is the aging time.

The moisture diffusion equations of phases 1–3 are:

$$\frac{\partial C_1(x,t)}{\partial t} = D_1 \frac{\partial^2 C_1(x,t)}{\partial x^2}, a_2 < x < a_1, t > 0 \quad (1)$$

$$\frac{\partial C_2(x,t)}{\partial t} = D_2 \frac{\partial^2 C_2(x,t)}{\partial x^2}, a_3 < x < a_2, t > 0 \quad (2)$$

$$\frac{\partial C_3(x, t)}{\partial t} = D_3 \frac{\partial^2 C_3(x, t)}{\partial x^2}, 0 < x < a_3, t > 0 \tag{3}$$

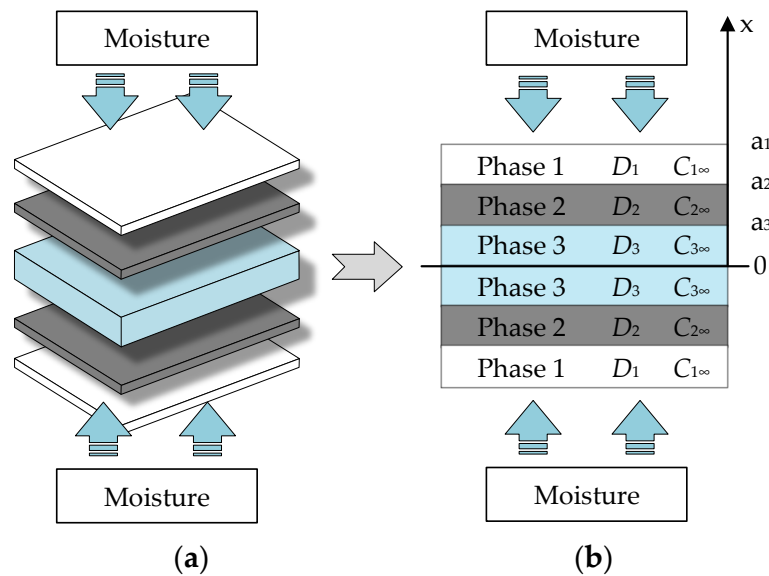


**Figure 1.** The moisture diffusion problem of multiphase symmetrical sandwich structure: (a) Description of multiphase symmetrical sandwich structure; (b) Model of moisture diffusion problem.

The boundary conditions are:

$$C_1(a_1, t) = C_{1\infty}, t \geq 0 \tag{4}$$

$$\frac{\partial C_3(0, t)}{\partial x} = 0, t \geq 0 \tag{5}$$

The initial conditions are:

$$C_1(x, 0) = 0, a_2 < x < a_1 \tag{6}$$

$$C_2(x, 0) = 0, a_3 < x < a_2 \tag{7}$$

$$C_3(x, 0) = 0, 0 < x < a_3 \tag{8}$$

The interface conditions are:

$$\frac{C_1(a_2, t)}{C_{1\infty}} = \frac{C_2(a_2, t)}{C_{2\infty}}, t \geq 0$$

$$D_1 \frac{\partial C_1(a_2, t)}{\partial x} = D_2 \frac{\partial C_2(a_2, t)}{\partial x}, t \geq 0 \tag{9}$$

$$\frac{C_2(a_3, t)}{C_{2\infty}} = \frac{C_3(a_3, t)}{C_{3\infty}}, t \geq 0$$

$$D_2 \frac{\partial C_2(a_3, t)}{\partial x} = D_3 \frac{\partial C_3(a_3, t)}{\partial x}, t \geq 0 \tag{10}$$

The Laplace transform of Equations (1)–(3) are:

$$\frac{\partial^2 \bar{C}_1(x, p)}{\partial x^2} - q_1^2 \bar{C}_1(x, p) = 0, a_2 < x < a_1 \tag{11}$$

$$\frac{\partial^2 \bar{C}_2(x, p)}{\partial x^2} - q_2^2 \bar{C}_2(x, p) = 0, a_3 < x < a_2 \tag{12}$$

$$\frac{\partial^2 \bar{C}_3(x, p)}{\partial x^2} - q_3^2 \bar{C}_3(x, p) = 0, 0 < x < a_3 \tag{13}$$

where  $q_i = (p/D_i)^{1/2}$ ,  $i = 1, 2, 3$ ,  $p$  is complex frequency. The solutions of Equations (11)–(13) are:

$$\bar{C}_1(x, p) = \frac{C_{1\infty}d_2}{pd_1} \tag{14}$$

$$\bar{C}_2(x, p) = \frac{2C_{2\infty}d_3}{pd_1} \tag{15}$$

$$\bar{C}_3(x, p) = \frac{4C_{3\infty} \cosh \mu(kk_1x)}{pd_1} \tag{16}$$

where  $\sigma = (kD_2/D_1)$ ,  $k = (D_1/D_2)^{1/2}$ ,  $C_{2\infty}/C_{1\infty} = r$ ,  $\sigma_1 = (k_1D_3/D_2)$ ,  $k_1 = (D_2/D_3)^{1/2}$ ,  $C_{3\infty}/C_{2\infty} = r_1$ ,  $\mu = (\lambda/D_1)^{1/2}$ ,  $d_1$ ,  $d_2$  and  $d_3$  are shown in Appendix A. Define  $\mu = i\beta_m$ , and  $\pm \beta_m$  ( $m = 1, 2, 3, \dots$ ) is the root of the following equation:

$$\begin{aligned} &(1 + \sigma_1r_1 + \sigma r + \sigma_1r_1\sigma r) \cos \mu((a_1 - a_2) + k(a_2 - a_3) + kk_1a_3) + \\ &(1 - \sigma_1r_1 + \sigma r - \sigma_1r_1\sigma r) \cos \mu((a_1 - a_2) + k(a_2 - a_3) - kk_1a_3) + \\ &(1 - \sigma_1r_1 - \sigma r + \sigma_1r_1\sigma r) \cos \mu((a_1 - a_2) - k(a_2 - a_3) + kk_1a_3) + \\ &(1 + \sigma_1r_1 - \sigma r - \sigma_1r_1\sigma r) \cos \mu((a_1 - a_2) - k(a_2 - a_3) - kk_1a_3) = 0 \end{aligned} \tag{17}$$

Thus, the solutions of concentrations in phase 1–3 are:

$$C_1(x, t) = C_{1\infty} \left( 1 - \sum_{m=1}^{\infty} \frac{2d_5}{\beta_m d_4} e^{-D_1 \beta_m^2 t} \right) \tag{18}$$

$$C_2(x, t) = C_{2\infty} \left( 1 - \sum_{m=1}^{\infty} \frac{2d_6}{\beta_m d_4} e^{-D_1 \beta_m^2 t} \right) \tag{19}$$

$$C_3(x, t) = C_{3\infty} \left( 1 - \sum_{m=1}^{\infty} \frac{2 \cos \beta_m(kk_1x)}{\beta_m d_4} e^{-D_1 \beta_m^2 t} \right) \tag{20}$$

where  $d_4$ ,  $d_5$  and  $d_6$  are shown in Appendix A. Then, the moisture absorptions of phase 1–3 are obtained by integral along the thickness direction:

$$M_1(t) = \int_{a_2}^{a_1} C_1(x, t) dx = C_{1\infty} \left( a_1 - a_2 - \sum_{m=1}^{\infty} \frac{2d_7}{\beta_m^2 d_4} e^{-D_1 \beta_m^2 t} \right) \tag{21}$$

$$M_2(t) = \int_{a_3}^{a_2} C_2(x, t) dx = C_{2\infty} \left( a_2 - a_3 - \sum_{m=1}^{\infty} \frac{2d_8}{k\beta_m^2 d_4} e^{-D_1 \beta_m^2 t} \right) \tag{22}$$

$$M_3(t) = \int_0^{a_3} C_3(x, t) dx = C_{3\infty} \left( a_3 - \sum_{m=1}^{\infty} \frac{2 \sin \beta_m kk_1 a_3}{kk_1 \beta_m^2 d_4} e^{-D_1 \beta_m^2 t} \right) \tag{23}$$

where  $d_7$  and  $d_8$  are shown in Appendix A. Thus, the total moisture uptake of sandwich structure is:

$$M_{total}(t) = 2M_1(t) + 2M_2(t) + 2M_3(t) \tag{24}$$

### 3. Experiment

Unidirectional glass fiber fabric was provided by Nanjing glass fiber research institute, unidirectional flax fiber fabric and jute fiber plane weave fabric were processed and manufactured by Nanjing Haituo composite material Co., Ltd., as shown in Figure 2a–c. The fiber fabric density and fiber density are given in Table 1. Non-hybrid and hybrid composite materials were formed by mold pressing, flax, glass and jute fiber fabrics. They were arranged on thick steel plates, and fabrics were manufactured according to the same fiber direction but according to a different layer sequence. The manufacturing process is illustrated in Figure 2d. Then, the composites were cured at room temperature after vac-

uum pumping experiment. Finally, the composite plates were cut into moisture absorption specimens by a cutting machine; the specimen is shown in Figure 2e. There were three test pieces of each composite type. The layer sequence and thickness of flax/glass/jute fiber-reinforced sandwich structures are shown in Table 2.

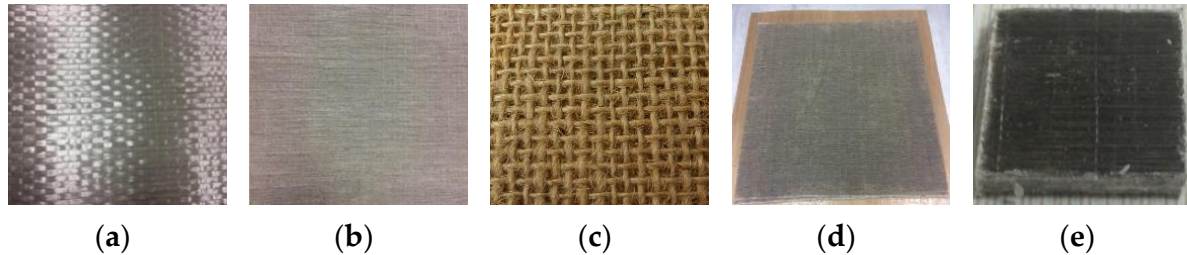


**Figure 2.** The material used in moisture absorption experiment. (a) Glass fiber fabric; (b) Flax fiber fabric; (c) Jute fiber plane weave fabric; (d) The manufacture process of composites; (e) Specimen.

**Table 1.** The density of fiber fabric and fiber.

Materials	Glass	Flax	Jute
Fiber fabric density	200 g/m <sup>2</sup>	200 g/m <sup>2</sup>	350 g/m <sup>2</sup>
Fiber density	2600 kg/m <sup>3</sup>	1400 kg/m <sup>3</sup>	1460 kg/m <sup>3</sup>

**Table 2.** The parameters of different layer sequence.

Composite	Number of Layers (Flax/Glass/Jute)	Layer Structure	Thickness (mm) (Flax/Glass/Jute)
F8	8/0/0	FFFFFFFF	3.68/0/0
J4	0/0/4	JJJJ	0/3.36/0
G8	0/8/0	GGGGGGGG	0/1.76/0
[F2/G2] <sub>s</sub>	4/4/0	FFGGGGFF	1.84/0.88/0
[F/G3] <sub>s</sub>	2/6/0	FGGGGGGF	0.92/1.32/0
[FGGF] <sub>s</sub>	4/4/0	FGGFFGGF	1.84/0.88/0
[FG] <sub>s</sub>	2/2/2	FGJJGF	0.92/0.88/1.68

F: Flax layer, G: Glass layer, J: Jute layer s: symmetrical.

The moisture absorption test pieces of sandwich structural composites were firstly put into a 60 °C constant temperature drying oven for 24 h, then the specimens were taken out and the four lateral sides of the moisture absorption test pieces were coated with waterproof material to ensure that the moisture diffuses along the thickness direction during the moisture absorption test. Next, the moisture absorption of specimens was tested by an electronic balance (Mettler Toledo al-104) and we recorded the initial mass  $W_0$  of the dried test piece. Then, the specimens were put into a constant temperature environmental box with 60 °C and 100% relative humidity. The specimens were taken out at a certain time, wiped with the test paper, and their weight gains  $W_t$  were weighed and recorded until the moisture absorption basically does not increase. The moisture absorption  $M_t$  of the material is expressed by the following formula:

$$M_t = \frac{W_t - W_0}{W_0} \times 100\% \tag{25}$$

The diffusivity can be calculated as below:

$$D = \pi \left( \frac{hk}{4M_\infty} \right)^2 \tag{26}$$

where  $h$  is the specimen thickness,  $D$  is the diffusivity and  $M_\infty$  is its maximum moisture uptake in equilibrium state.  $k$  is the slope of the linear part of  $M_t$  versus the  $t^{0.5}$  curve [25].

### 4. Finite Element Analysis

The moisture diffusion of multiphase symmetrical sandwich structures through the thickness direction were solved by the analytical method. To validate the analytical model, the sandwich structure including phase 1–3 was developed in the commercial software Abaqus 6.11. The model established in Abaqus is shown in Figure 3. The mass diffusion method in Abaqus is Fick’s second law ( $\partial\psi/\partial t = D\partial^2\psi/\partial x^2$ ), which predicts how diffusion causes the concentration to change with time, where  $\psi$  represents normalized concentration. A mass diffusion option was used when the materials and steps in Abaqus were set up. Because Abaqus does not have the element type for moisture diffusion in family option, we used heat transfer element instead. The number of mesh element is 400, the element type is a 4-node linear heat transfer quadrilateral. The element type is shown in Figure 4. The boundary condition of analytical method is normalized concentration = 1. This boundary condition is also used in moisture diffusion experiment since water or humid = 100% environment was treated as normalized concentration = 1 at the surface of specimens in experiment. Thus, normalized concentration = 1 was applied at the upper and bottom surfaces.

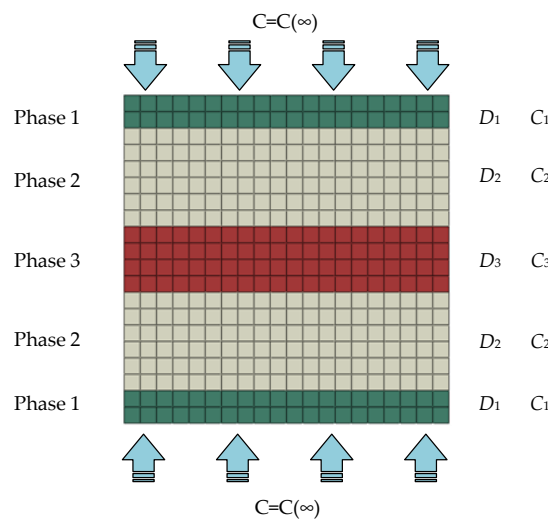


Figure 3. The FEA model for multiphase symmetrical sandwich structure.

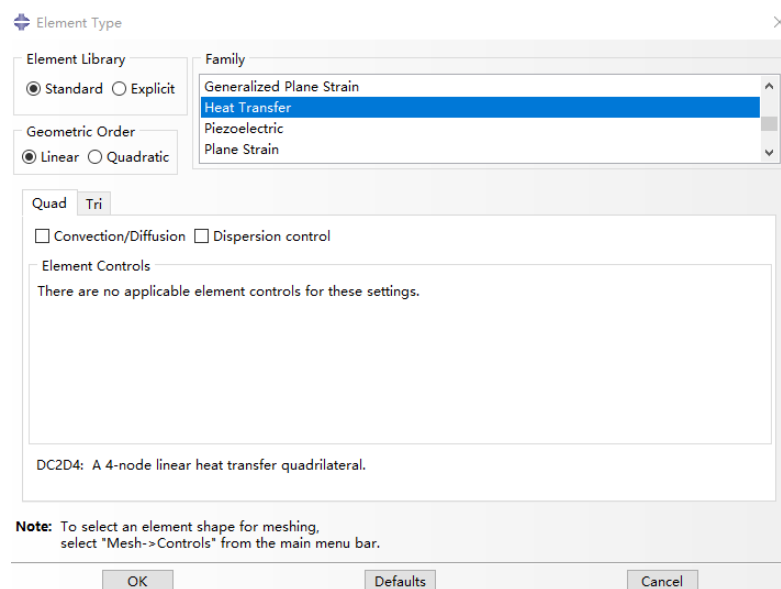


Figure 4. The element type of moisture diffusion model in Abaqus.



The parameters including thickness (mm), the diffusivity (mm<sup>2</sup>/h) and equilibrium moisture content (%) in this structure are defined, and four cases are shown in Table 3.

**Table 3.** The parameters in FEA model.

Case	$a_1$	$a_2$	$a_3$	$D_1$	$C_1$	$D_2$	$C_2$	$D_3$	$C_3$
Case 1	0.5	0.4	0.1	0.001	1	0.0005	0.5	0.0003	0.3
Case 2	0.5	0.2	0.1	0.001	1	0.0005	0.5	0.0003	0.3
Case 3	0.5	0.4	0.1	0.0003	0.3	0.0005	0.5	0.001	1
Case 4	0.5	0.2	0.1	0.0003	0.3	0.0005	0.5	0.001	1

## 5. Result and Discussion

### 5.1. FEA Validation

Figure 5 illustrates the moisture uptake comparison of cases 1–4 between analytical results and FEA calculation. Four cases of moisture absorption for multiphase symmetrical sandwich structure were calculated by Abaqus, the thicknesses, diffusivities, and equilibrium moisture contents of phases 1–3 were changed to verify the analytical method by Equation (24). In reference [25], we know that the initial moisture uptake is a straight line for Fickian diffusion if we use  $t^{0.5}$  as the  $x$ -axis. To conveniently observe whether the moisture is Fickian diffusion,  $t^{0.5}$  or  $t^{0.5}/h$  is often used as  $x$ -axis [25,26,31]. Here, we use  $t^{0.5}/h$  as  $x$ -axis. The unit of thickness  $h$  is mm and the unit of time  $t$  is hour. Compared with the FEA calculation, the analytical results show a good agreement.

### 5.2. The Effect of Interface Condition

The interface condition will play a very important role for the final results of moisture absorption. By using analytical methods here, we will explain the details of concentration at the interface. For example, the concentration and normalized concentration distributions at the interface of case 1 are shown in Figures 6 and 7. The concentration distributions were calculated by Abaqus, and depicted at  $t = 0$  h, 20 h, 200 h, 800 h. Figures 6a and 7a represent that both concentration and normalized concentration at  $t = 0$  h are 0, however, when  $t = 20$  h, the normalized concentration is continuous while concentration is discontinuous, this phenomenon is shown in Figures 6b and 7b. When  $t = 200$  h and  $t = 800$  h, we can find clearly results that the normalized concentration at the interface is still continuous. However, concentration is totally discontinuous, as illustrated in Figure 6c,d and Figure 7c,d. To better conclude the difference between concentration and normalized concentration, we give FEA comparison results when  $t = 800$  h as shown in Figure 8. From this picture, it is obvious that the concentrations have a jump value (1 vs. 0.5, 0.5 vs. 0.3) at the interface, while the normalized concentration is continuous (1 vs. 0.999, 0.998 vs. 0.997). Thus, the normalized concentration continuity condition can more accurately describe the concentration distribution sandwich structure.

To better understand concentration  $C$  and normalized concentration  $\psi$ , the explanation is shown as follow. The concentration  $C$  is defined as  $C = M/V$ , where  $M$  is moisture uptake and  $V$  is volume of the sample. The normalized concentration  $\psi = C/C_\infty$ . Obviously, the saturated moisture concentration  $C_\infty$  and  $V$  may be different from each other for different phases, but the normalized concentration  $\psi$  will finally reach 1. Thus, the normalized concentration is continuous, while concentration is discontinuous.

### 5.3. Comparison between Experimental and Analytical Results

Figure 9 shows the analytical and experimental results of weight gains of [FFFF]<sub>S</sub>, [JJ]<sub>S</sub>, [FFGG]<sub>S</sub>, [FGGG]<sub>S</sub>, [GGGG]<sub>S</sub>, [FG]<sub>S</sub>, and [FGGF]<sub>S</sub>. The moisture diffusion parameters of single layer flax fiber composite, glass fiber composite and jute fiber composite can be obtained from the moisture uptake curve of [FFFF]<sub>S</sub>, [GGGG]<sub>S</sub> and [JJ]<sub>S</sub>, and the values are given in Table 4. It can be found from Figure 9 that the analytical values calculated by the moisture diffusion model were in good agreement with the experimental results for different layer sequences, [FFGG]<sub>S</sub>, [FGGG]<sub>S</sub>, [FG]<sub>S</sub>, and [FGGF]<sub>S</sub>. The experimental

results of [FFGG]<sub>S</sub> and [FGGG]<sub>S</sub> represent two-phase moisture diffusion cases; it was proven that the proposed model can also deal with two-phase moisture diffusion cases. The experimental cases of [FG]<sub>S</sub> and [FGGF]<sub>S</sub> were also carried out to validate the moisture diffusion cases, and the good results were achieved.

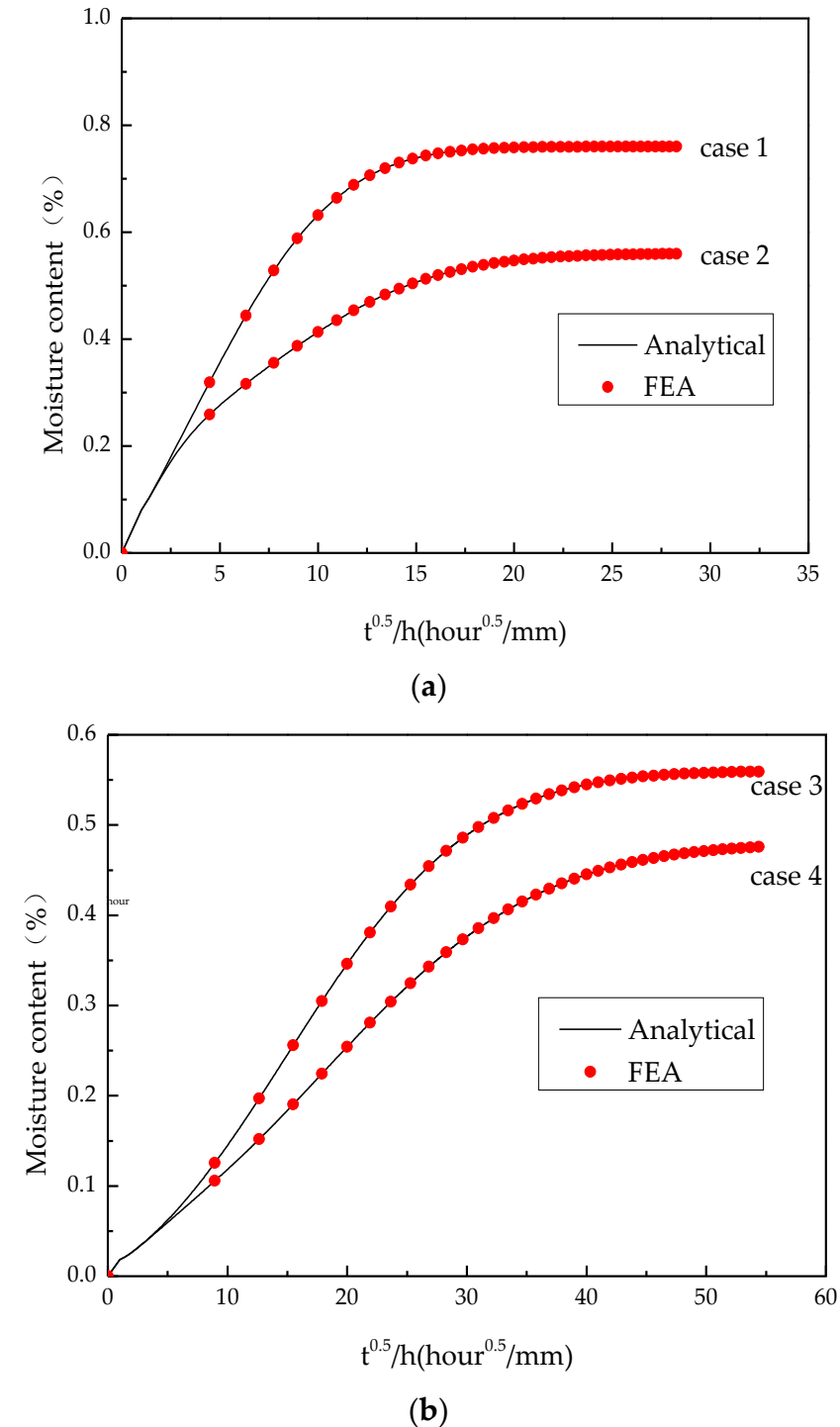


**Figure 5.** The comparison between analytical and FEA results, (a) Case 1 and case 2; (b) Case 3 and case 4.

From Figure 9a, it is also found that the moisture diffusion behavior of [FFFF]<sub>S</sub>, [JJ]<sub>S</sub>, [FFGG]<sub>S</sub>, [FGGG]<sub>S</sub> and [GGGG]<sub>S</sub>, which are single material structures and two-phase structures, basically match Fick’s second law. The saturated moisture absorptions of the



composites were obtained by the experimental results of [FFFF]<sub>S</sub>, [JJ]<sub>S</sub> and [GGGG]<sub>S</sub>. The saturated moisture uptake of [FFFF]<sub>S</sub> (8.60%) is about eight times than that of [GGGG]<sub>S</sub> (1.05%). The moisture diffusivities of [FFFF]<sub>S</sub> (0.0165 mm<sup>2</sup>/h) is about five times than that of [GGGG]<sub>S</sub> (0.0031 mm<sup>2</sup>/h). The moisture diffusion parameters of jute fiber reinforced composite are similar with flax fiber reinforced composite, its saturated moisture uptake is 7.09%, and its diffusivity is 0.00142 mm<sup>2</sup>/h. The saturated moisture uptake of sandwich structural composites decreases significantly with the increase of glass fiber, for example, [FFGG]<sub>S</sub> and [FGGG]<sub>S</sub> are 58% and 35% of the saturated moisture absorption of [FFFF]<sub>S</sub>. The reason is attributed to the fact that the glass fiber is non-hygroscopic while flax fiber is highly hydrophilic. Figure 9b shows the weight gain curve of [FGJ]<sub>S</sub> and [FGGF]<sub>S</sub> structures. From the figure, it can be seen that the moisture diffusion behaviors of these sandwich structures no longer fit Fick’s law: their weight gains rapidly increase at first, then slowly increase until saturation. This phenomenon occurs because there are “FGGF” and “FGJ” structures in the ply, and the moisture diffuses faster in the flax fiber layer on the surface and inside, while the glass fiber layer in the middle diffuses slower.

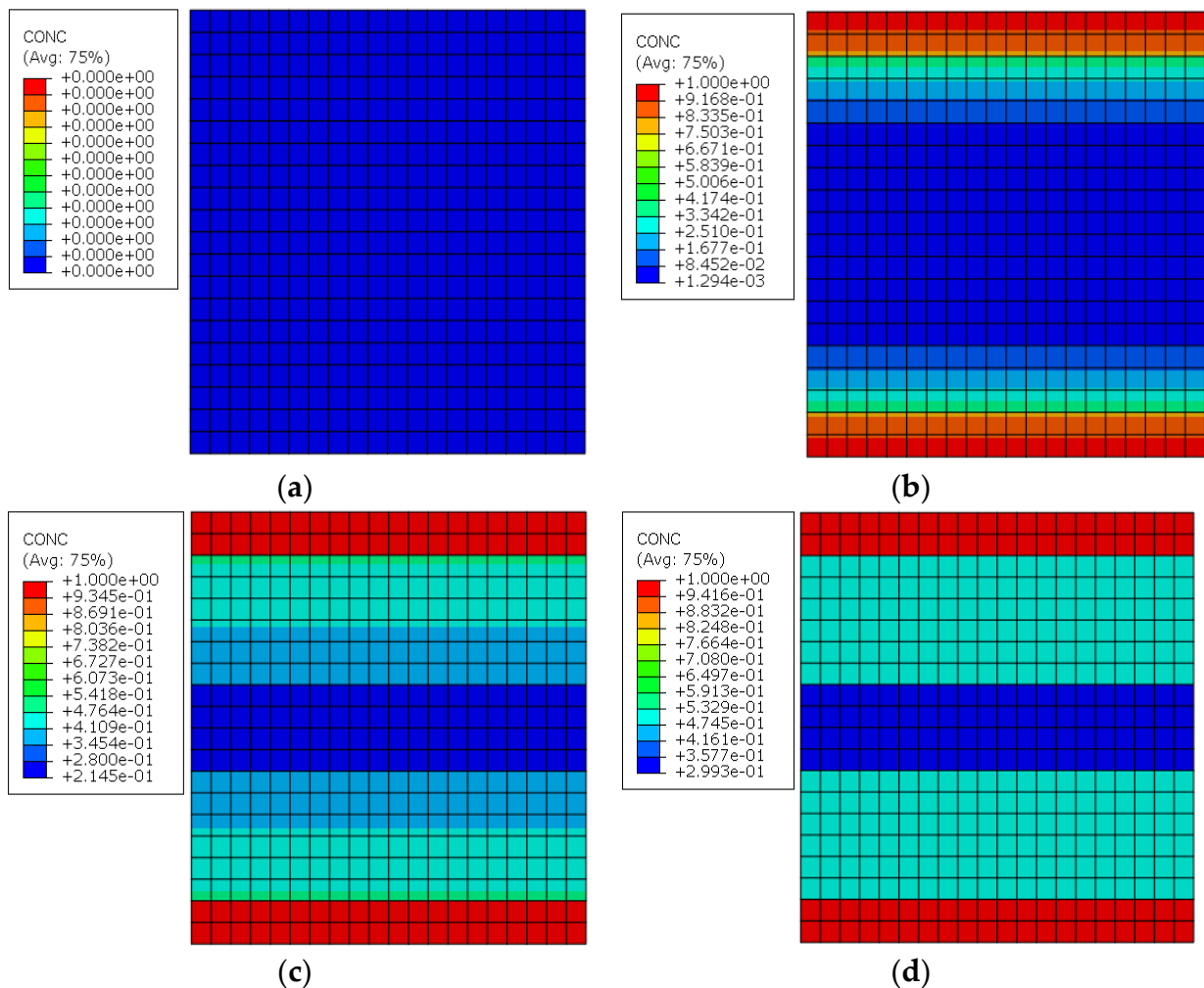


Figure 6. The concentration distribution of sandwich structure: (a)  $t = 0$  h; (b)  $t = 20$  h; (c)  $t = 200$  h; (d)  $t = 800$  h.

Table 4. The diffusivity and saturated moisture content of flax, glass and jute fiber fabric.

Parameters	FFRP	CFRP	JFRP
Diffusivity (mm <sup>2</sup> /h)	0.0165	0.0031	0.0142
Saturated moisture content (%)	8.60%	1.05%	7.09%

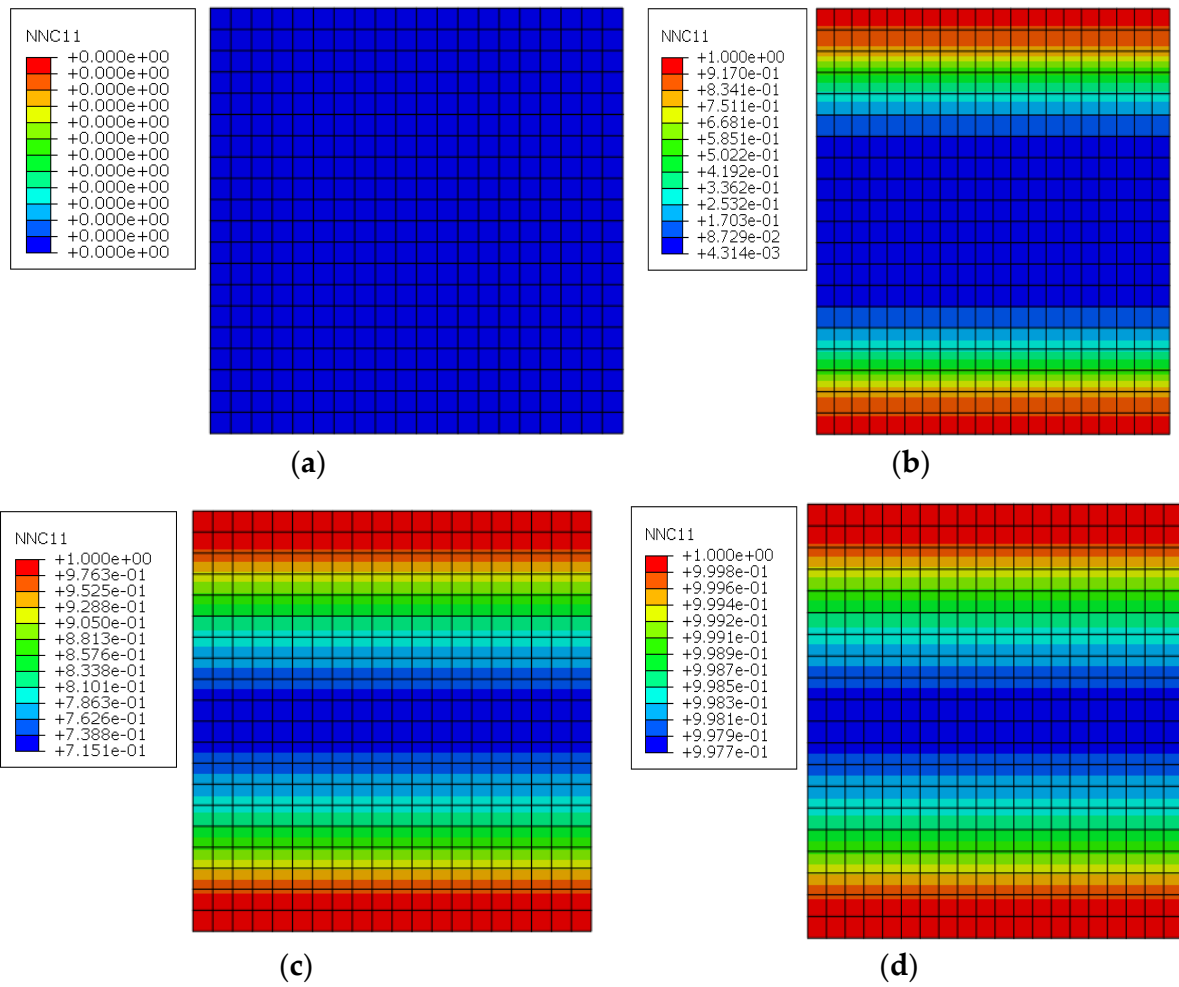


Figure 7. The normalized concentration distribution of sandwich structure: (a)  $t = 0$  h; (b)  $t = 20$  h; (c)  $t = 200$  h; (d)  $t = 800$  h.

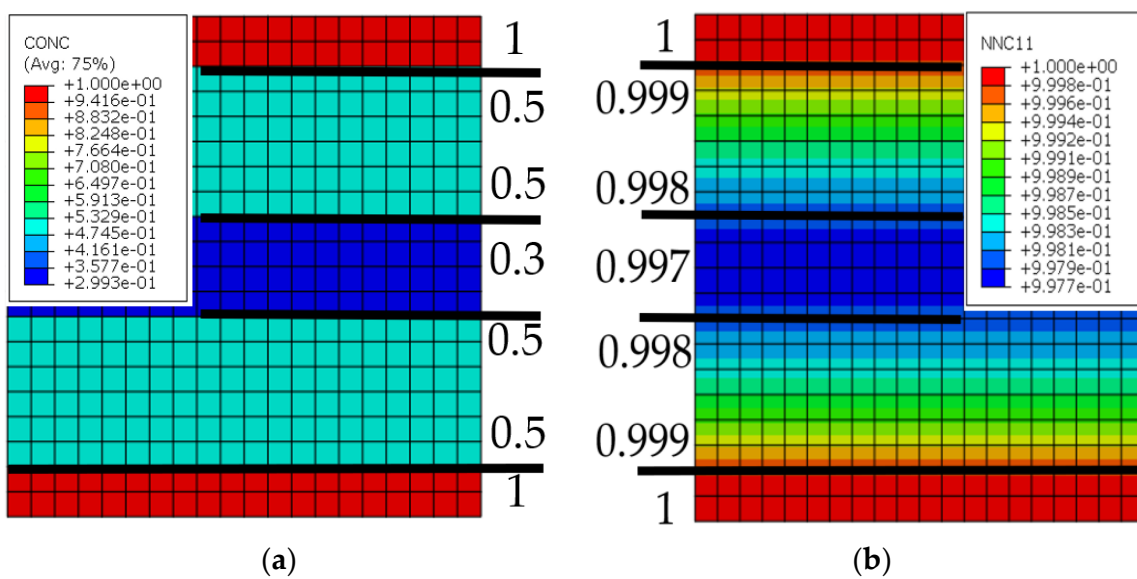
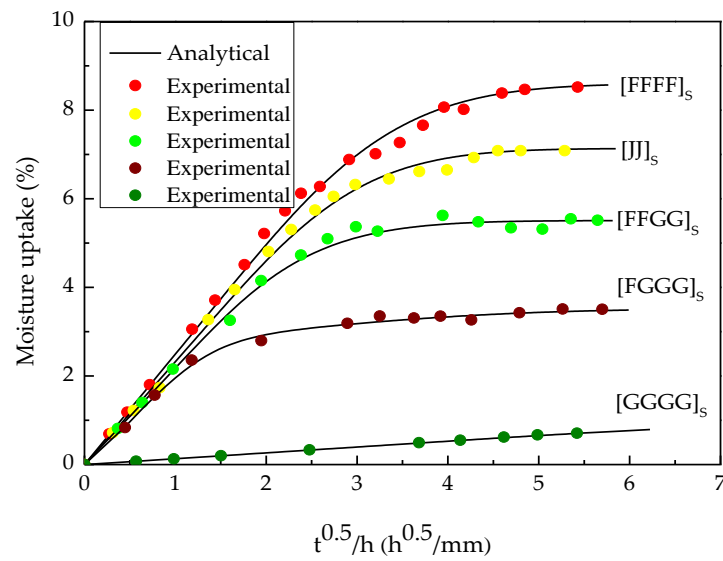
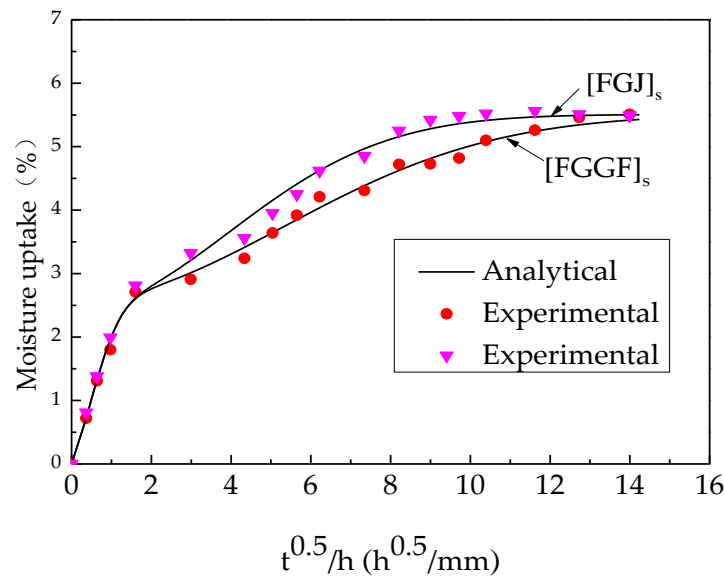


Figure 8. The details of finally concentration distribution of sandwich structure: (a) Concentration distribution; (b) Normalized concentration distribution.



(a)



(b)

**Figure 9.** The details of final concentration distribution of sandwich structure: (a) Concentration distribution; (b) Normalized concentration distribution.

The root mean square error (RMSE) between analytical and experimental results is shown in Table 5. From Table 5, it is seen that RMSE of [FFGG], [FGGG], [FGJ], and [FGGF] is less than 0.130. The errors between analytical and experimental results are small enough to prove obtained analytical results.

**Table 5.** The RMSE between analytical and experimental results.

Material	FFGG	FGGG	FGJ	FGGF
RSME	0.130	0.071	0.126	0.102

### 6. Conclusions

This paper presents a solution of moisture diffusion equations for multiphase symmetrical sandwich structures. Both the FEA and experimental works have been carried out to validate the analytical results, and the main conclusions are listed below:

1. The analytical solution of moisture diffusion equation was given to predict the moisture absorption of multiphase symmetrical sandwich structures; the diffusivities and saturated moisture concentrations of different phases in sandwich structure can be obtained according to moisture diffusion experiments of non-hybrid fiber reinforced composites. Compared with FEA and other methods, the analytical solution of moisture uptake or concentration can be used as basic variables to further analyze the stress or strength of multiphase symmetrical sandwich structures when they are exposed to hydrothermal environments. The analytical solution is more convenient and intuitive.
2. FEA results were obtained using a mass diffusion method in Abaqus, the validation of analytical method by FEA was carried out for four cases, and the results show a good agreement.
3. The interface condition of different phases in sandwich structure was discussed. The concentration and normalized concentration at the interface were compared by FEA results. The fact was obtained that the normalized concentration is continuous at the interface. Thus, the correct interface conditions are continuous normalized concentration conditions.
4. The moisture absorption experiments of flax/glass/jute-reinforced epoxy composites with different layer configurations were carried out to validate the analytical application, the experiments contained two-phase and three-phase cases, and the analytical predictions matched the experimental results.

**Author Contributions:** Conceptualization, H.Y. and L.Y.; methodology, H.Y.; software, Y.M.; validation, Z.H.; formal analysis, J.T.; investigation, Y.W.; resources, Y.N.; data curation, L.Y.; writing—original draft preparation, H.Y.; writing—review and editing, H.Y.; visualization, H.Y.; supervision, L.Y.; project administration, L.Y.; funding acquisition, L.Y. All authors have read and agreed to the published version of the manuscript.

**Funding:** This research was funded by the National Natural Science Foundation of China under Grant 52105153, in part by the Natural Science Foundation of the Jiangsu Higher Education Institutions of China under Grants 22KJA540001, 21KJB570009, 19KJB430029, and 20KJA540001, in part by Projects from Nantong city Grant MS2021005, MS22021003, MS22021022, JC2021041 and JC2021060, in part by Collaborative Innovation Fund Project of Jiangsu Advanced Textile Engineering Technology Center under Grant XJFZ/2021/16, in part by Key Laboratory of Yarn Materials Forming and Composite Processing Technology, Zhejiang Province under Grant MTC2021-06.

**Institutional Review Board Statement:** Not applicable.

**Informed Consent Statement:** Not applicable.

**Data Availability Statement:** Not applicable.

**Conflicts of Interest:** The authors declare no conflict of interest.

## Abbreviations

### Nomenclatures

$C$	Concentration, g/L
$D$	Diffusivity, $\text{mm}^2/\text{h}$
$t$	Time, h
$a$	Thickness, mm
$C_\infty$	Saturated moisture concentration, g/L
$M$	Moisture content, %
$M_\infty$	Saturated moisture content, %
$V$	Volume of the sample, $\text{mm}^3$
$h$	Thickness of the specimen, mm
$W_t$	Weight gains of the specimen with the time, g
$W_0$	Initial mass of the specimen, g
$\Psi$	Normalized concentration, non-dimension
$\beta_m$	The root of characteristic equation, non-dimension

**Abbreviations**

FEA	Finite Element Analysis
FFRP	Flax Fiber Reinforced Plastic
CFR	Carbon Fiber Reinforced Plastic
JFRP	Jute Fiber Reinforced Plastic

**Appendix A**

$$\begin{aligned}
 d_1 = & (1 + \sigma_1 r_1 + \sigma r + \sigma_1 r_1 \sigma r) \cosh \mu((a_1 - a_2) + k(a_2 - a_3) + kk_1 a_3) + \\
 & (1 - \sigma_1 r_1 + \sigma r - \sigma_1 r_1 \sigma r) \cosh \mu((a_1 - a_2) + k(a_2 - a_3) - kk_1 a_3) + \\
 & (1 - \sigma_1 r_1 - \sigma r + \sigma_1 r_1 \sigma r) \cosh \mu((a_1 - a_2) - k(a_2 - a_3) + kk_1 a_3) + \\
 & (1 + \sigma_1 r_1 - \sigma r - \sigma_1 r_1 \sigma r) \cosh \mu((a_1 - a_2) - k(a_2 - a_3) - kk_1 a_3)
 \end{aligned} \tag{A1}$$

$$\begin{aligned}
 d_2 = & (1 + \sigma_1 r_1 + \sigma r + \sigma_1 r_1 \sigma r) \cosh \mu((x - a_2) + k(a_2 - a_3) + kk_1 a_3) + \\
 & (1 - \sigma_1 r_1 + \sigma r - \sigma_1 r_1 \sigma r) \cosh \mu((x - a_2) + k(a_2 - a_3) - kk_1 a_3) + \\
 & (1 - \sigma_1 r_1 - \sigma r + \sigma_1 r_1 \sigma r) \cosh \mu((x - a_2) - k(a_2 - a_3) + kk_1 a_3) + \\
 & (1 + \sigma_1 r_1 - \sigma r - \sigma_1 r_1 \sigma r) \cosh \mu((x - a_2) - k(a_2 - a_3) - kk_1 a_3)
 \end{aligned} \tag{A2}$$

$$\begin{aligned}
 d_3 = & (1 + \sigma_1 r_1) \cosh \mu(k(x - a_3) + kk_1 a_3) + \\
 & (1 - \sigma_1 r_1) \cosh \mu(k(x - a_3) - kk_1 a_3)
 \end{aligned} \tag{A3}$$

$$\begin{aligned}
 d_4 = & (1 + \sigma_1 r_1 + \sigma r + \sigma_1 r_1 \sigma r)((a_1 - a_2) + k(a_2 - a_3) + kk_1 a_3) * \\
 & \sin \beta_m((a_1 - a_2) + k(a_2 - a_3) + kk_1 a_3) + \\
 & (1 - \sigma_1 r_1 + \sigma r - \sigma_1 r_1 \sigma r)((a_1 - a_2) + k(a_2 - a_3) - kk_1 a_3) * \\
 & \sin \beta_m((a_1 - a_2) + k(a_2 - a_3) - kk_1 a_3) + \\
 & (1 - \sigma_1 r_1 - \sigma r + \sigma_1 r_1 \sigma r)((a_1 - a_2) - k(a_2 - a_3) + kk_1 a_3) * \\
 & \sin \beta_m((a_1 - a_2) - k(a_2 - a_3) + kk_1 a_3) + \\
 & (1 + \sigma_1 r_1 - \sigma r - \sigma_1 r_1 \sigma r)((a_1 - a_2) - k(a_2 - a_3) - kk_1 a_3) * \\
 & \sin \beta_m((a_1 - a_2) - k(a_2 - a_3) - kk_1 a_3)
 \end{aligned} \tag{A4}$$

$$\begin{aligned}
 d_5 = & (1 + \sigma_1 r_1 + \sigma r + \sigma_1 r_1 \sigma r) \cos \beta_m((x - a_2) + k(a_2 - a_3) + kk_1 a_3) + \\
 & (1 - \sigma_1 r_1 + \sigma r - \sigma_1 r_1 \sigma r) \cos \beta_m((x - a_2) + k(a_2 - a_3) - kk_1 a_3) + \\
 & (1 - \sigma_1 r_1 - \sigma r + \sigma_1 r_1 \sigma r) \cos \beta_m((x - a_2) - k(a_2 - a_3) + kk_1 a_3) + \\
 & (1 + \sigma_1 r_1 - \sigma r - \sigma_1 r_1 \sigma r) \cos \beta_m((x - a_2) - k(a_2 - a_3) - kk_1 a_3)
 \end{aligned} \tag{A5}$$

$$\begin{aligned}
 d_6 = & (1 + \sigma_1 r_1) \cos \beta_m(k(x - a_3) + kk_1 a_3) + \\
 & (1 - \sigma_1 r_1) \cos \beta_m(k(x - a_3) - kk_1 a_3)
 \end{aligned} \tag{A6}$$

$$\begin{aligned}
 d_7 = & (1 + \sigma_1 r_1 + \sigma r + \sigma_1 r_1 \sigma r) \sin \beta_m((a_1 - a_2) + k(a_2 - a_3) + kk_1 a_3) + \\
 & (1 - \sigma_1 r_1 + \sigma r - \sigma_1 r_1 \sigma r) \sin \beta_m((a_1 - a_2) + k(a_2 - a_3) - kk_1 a_3) + \\
 & (1 - \sigma_1 r_1 - \sigma r + \sigma_1 r_1 \sigma r) \sin \beta_m((a_1 - a_2) - k(a_2 - a_3) + kk_1 a_3) + \\
 & (1 + \sigma_1 r_1 - \sigma r - \sigma_1 r_1 \sigma r) \sin \beta_m((a_1 - a_2) - k(a_2 - a_3) - kk_1 a_3) - \\
 & [(1 + \sigma_1 r_1 + \sigma r + \sigma_1 r_1 \sigma r) \sin \beta_m(k(a_2 - a_3) + kk_1 a_3) + \\
 & (1 - \sigma_1 r_1 + \sigma r - \sigma_1 r_1 \sigma r) \sin \beta_m(k(a_2 - a_3) - kk_1 a_3) + \\
 & (1 - \sigma_1 r_1 - \sigma r + \sigma_1 r_1 \sigma r) \sin \beta_m(-k(a_2 - a_3) + kk_1 a_3) + \\
 & (1 + \sigma_1 r_1 - \sigma r - \sigma_1 r_1 \sigma r) \sin \beta_m(-k(a_2 - a_3) - kk_1 a_3)]
 \end{aligned} \tag{A7}$$

$$\begin{aligned}
 d_8 = & (1 + \sigma_1 r_1) \sin \beta_m(k(a_2 - a_3) + kk_1 a_3) + \\
 & (1 - \sigma_1 r_1) \sin \beta_m(k(a_2 - a_3) - kk_1 a_3) - 2 \sin \beta_m k k_1 a_3
 \end{aligned} \tag{A8}$$

## References

1. Guo, Y.; Qiu, H.; Ruan, K.; Wang, S.; Zhang, Y.; Gu, J. Flexible and insulating silicone rubber composites with sandwich structure for thermal management and electromagnetic interference shielding. *Compos. Sci. Technol.* **2022**, *219*, 109253. [\[CrossRef\]](#)
2. Zhang, Y.; Yan, L.; Zhang, C.; Guo, S. Low-velocity impact response of tube-reinforced honeycomb sandwich structure. *Thin-Walled Struct.* **2021**, *158*, 107188. [\[CrossRef\]](#)
3. Zhao, W.; Liu, Z.; Yu, G.; Wu, L. A new multifunctional carbon fiber honeycomb sandwich structure with excellent mechanical and thermal performances. *Compos. Struct.* **2021**, *274*, 114306. [\[CrossRef\]](#)
4. Zhang, J.; Yan, Z.; Xia, L. Vibration and Flutter of a Honeycomb Sandwich Plate with Zero Poisson's Ratio. *Mathematics* **2021**, *9*, 2528. [\[CrossRef\]](#)
5. Yu, H.; Yang, J. Predictions of Moisture Diffusion Behavior of Cellulose-Fiber-Reinforced Plain Weave Epoxy Composites. *Polymers* **2021**, *13*, 2347. [\[CrossRef\]](#) [\[PubMed\]](#)
6. Fiore, V.; Calabrese, L.; Scalici, T.; Valenza, A. Evolution of the bearing failure map of pinned flax composite laminates aged in marine environment. *Compos. Part B Eng.* **2020**, *187*, 107864. [\[CrossRef\]](#)
7. Frydrych, M.; Hýsek, Š.; Fridrichová, L.; Le Van, S.; Herlík, M.; Pechočiaková, M.; Le Chi, H.; Louda, P. Impact of Flax and Basalt Fibre Reinforcement on Selected Properties of Geopolymer Composites. *Sustainability* **2020**, *12*, 118. [\[CrossRef\]](#)
8. Ali, A.; Shaker, K.; Nawab, Y.; Jabbar, M.; Hussain, T.; Militky, J.; Baheti, V. Hydrophobic treatment of natural fibers and their composites—A review. *J. Ind. Text.* **2018**, *47*, 2153–2183. [\[CrossRef\]](#)
9. Asim, M.; Jawaid, M.; Abdan, K.; Ishak, M. The effect of silane treated fibre loading on mechanical properties of pineapple leaf/kenaf fibre filler phenolic composites. *J. Polym. Environ.* **2018**, *26*, 1520–1527. [\[CrossRef\]](#)
10. Sanjay, M.; Madhu, P.; Jawaid, M.; Senthamaraiannan, P.; Senthil, S.; Pradeep, S. Characterization and properties of natural fiber polymer composites: A comprehensive review. *J. Clean. Prod.* **2018**, *172*, 566–581. [\[CrossRef\]](#)
11. Sepe, R.; Bollino, F.; Boccarusso, L.; Caputo, F. Influence of chemical treatments on mechanical properties of hemp fiber reinforced composites. *Compos. Part B Eng.* **2018**, *133*, 210–217. [\[CrossRef\]](#)
12. Baley, C.; Gomina, M.; Breard, J.; Bourmaud, A.; Davies, P. Variability of mechanical properties of flax fibres for composite reinforcement. A review. *Ind. Crops Prod.* **2019**, *145*, 111984. [\[CrossRef\]](#)
13. Jeannin, T.; Gabrion, X.; Ramasso, E.; Placet, V. About the fatigue endurance of unidirectional flax-epoxy composite laminates. *Compos. Part B Eng.* **2019**, *165*, 690–701. [\[CrossRef\]](#)
14. Radkar, S.S.; Amiri, A.; Ulven, C.A. Tensile Behavior and Diffusion of Moisture through Flax Fibers by Desorption Method. *Sustainability* **2019**, *11*, 3558. [\[CrossRef\]](#)
15. Saidane, E.H.; Scida, D.; Assarar, M.; Ayad, R. Assessment of 3D moisture diffusion parameters on flax/epoxy composites. *Compos. Part A* **2016**, *80*, 53–60. [\[CrossRef\]](#)
16. Nurge, M.A.; Youngquist, R.C.; Starr, S.O. Mass conservation in modeling moisture diffusion in multi-layer composite and sandwich structures. *J. Sandw. Struct. Mater.* **2010**, *12*, 755–763. [\[CrossRef\]](#)
17. Katzman, H.A.; Castaneda, R.M.; Lee, H.S. Moisture diffusion in composite sandwich structures. *Compos. Part A Appl. Sci. Manuf.* **2008**, *39*, 887–892. [\[CrossRef\]](#)
18. Kareem Jalghaf, H.; Omle, I.; Kovács, E. A Comparative Study of Explicit and Stable Time Integration Schemes for Heat Conduction in an Insulated Wall. *Buildings* **2022**, *12*, 824. [\[CrossRef\]](#)
19. Li, Y.-T.; Chen, H.; Deng, R.; Wu, M.-B.; Yang, H.-C.; Darling, S.B. Sandwich-structured photothermal wood for durable moisture harvesting and pumping. *ACS Appl. Mater. Interfaces* **2021**, *13*, 33713–33721. [\[CrossRef\]](#)
20. Wu, Y.; Pastor, M.-L.; Perrin, M.; Casari, P.; Gong, X. A new methodology to predict moisture effects on mechanical behaviors of GFRP-BALSA sandwich by acoustic emission and infrared thermography. *Compos. Struct.* **2022**, *287*, 115342. [\[CrossRef\]](#)
21. Najafi, M.; Darvizeh, A.; Ansari, R. Characterization of moisture effects on novel agglomerated cork core sandwich composites with fiber metal laminate facesheets. *J. Sandw. Struct. Mater.* **2020**, *22*, 1709–1742. [\[CrossRef\]](#)
22. Reddy, C.N.; Rajeswari, C.; Malyadri, T.; Hari, S.S. Effect of moisture absorption on the mechanical properties of jute/glass hybrid sandwich composites. *Mater. Today Proc.* **2021**, *45*, 3307–3311. [\[CrossRef\]](#)
23. Yu, H.; Zhou, C. Sandwich diffusion model for moisture absorption of flax/glass fiber reinforced hybrid composite. *Compos. Struct.* **2018**, *188*, 1–6. [\[CrossRef\]](#)
24. Joshi, N.; Muliana, A. Deformation in viscoelastic sandwich composites subject to moisture diffusion. *Compos. Struct.* **2010**, *92*, 254–264. [\[CrossRef\]](#)
25. Kondo, K.; Taki, T. Moisture diffusivity of unidirectional composites. *J. Compos. Mater.* **1982**, *16*, 82–93. [\[CrossRef\]](#)
26. Tang, X.; Whitcomb, J.D.; Li, Y.; Sue, H.-J. Micromechanics modeling of moisture diffusion in woven composites. *Compos. Sci. Technol.* **2005**, *65*, 817–826. [\[CrossRef\]](#)
27. Li, Y.; Zhu, Q. Simultaneous heat and moisture transfer with moisture sorption, condensation, and capillary liquid diffusion in porous textiles. *Text. Res. J.* **2003**, *73*, 515–524. [\[CrossRef\]](#)
28. Kim, N.-H. Moisture diffusion coefficients of a PE/PA composite membrane in an enthalpy exchanger for heat and moisture recovery. *J. Mech. Sci. Technol.* **2020**, *34*, 5295–5302. [\[CrossRef\]](#)
29. Chiba, R. An analytical solution for transient heat and moisture diffusion in a double-layer plate. In *Heat Transfer—Mathematical Modelling, Numerical Methods and Information Technology*; InTech Europe: Rijeka, Croatia, 2011; pp. 567–578.

30. Haghghi-Yazdi, M.; Lee-Sullivan, P. Modeling of structural mechanics, moisture diffusion, and heat conduction coupled with physical aging in thin plastic plates. *Acta Mech.* **2014**, *225*, 929–950. [[CrossRef](#)]
31. Bao, L.-R.; Yee, A.F. Moisture diffusion and hygrothermal aging in bismaleimide matrix carbon fiber composites: Part II—woven and hybrid composites. *Compos. Sci. Technol.* **2002**, *62*, 2111–2119. [[CrossRef](#)]
32. Fan, X. Mechanics of moisture for polymers: Fundamental concepts and model study. In Proceedings of the EuroSimE 2008—International Conference on Thermal, Mechanical and Multi-Physics Simulation and Experiments in Microelectronics and Micro-Systems, Freiburg im Breisgau, Germany, 20–23 April 2008; pp. 1–14.